Area moment of inertia of a “flower-shaped” cross section and generalization for *N*-fold rotational symmetry and multipole moments

Hans Jelitto

Institute of Advanced Ceramics, Hamburg University of Technology (TUHH), Germany,
December 10th, 2020,
E-mail: h.jelitto@tuhh.de, doi: 10.15480/882.3066

Abstract

Motivated by three-point bending tests with a nanoindenter and the necessary analysis, the area moment of inertia of tiny bending specimens, with a special “flower-shaped” cross section, is calculated analytically. If such cross sections have a four-fold rotational symmetry, it can be shown that a rotation of the cross section by any angle, with respect to the reference plane, does not change the result. By demonstrating that this is valid also for *N*-fold rotational symmetry with $N \geq 3$ and by generalization for multipole moments of any order, some interesting equations and principles are found. (Originally, the chapters 1–4 were an internal communication in the Institute of Advanced Ceramics, TUHH. Later on, the chapters 5–7 and the appendices were added, and the introduction was extended. Although the calculations are standard, they are perhaps also of interest to others. In order not to lose track of the idea and the calculations, they are published in this format.)

(Photo from Pixabay)

1. Introduction

In materials research and the development of new high-performance materials, the standard bending test remains one of the methods of choice for measuring mechanical properties. In order to calculate the stress, strength, Young's modulus (elastic modulus) and fracture toughness of materials in bending experiments, the area moment of inertia I is needed. The latter determines the "deflection under loading" or "resistance against bending", and it is calculated using the shape of the cross section of the bending sample. One bending method is three-point bending, which is schematically shown in Fig. 1, where w and h are the width and height of the sample, respectively, L is the distance between the support rollers and F is the force at the load point in the middle of the sample.

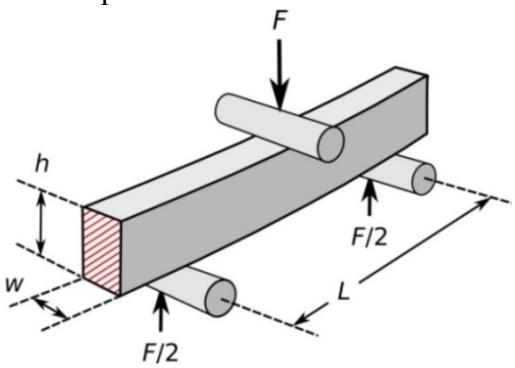

Fig. 1. Geometry of a specimen in three-point bending with the cross section shaded in red.

If the force continually increases, the sample will break in a certain moment and the maximum stress before fracture (in the middle of the tensile-loaded sample surface) is deemed the strength of the material. In three-point bending, the stress σ (strength) is given by [1]

$$\sigma = \frac{3FL}{2wh^2} \tag{1}$$

The area moment of inertia not only depends on the shape of the cross section (shaded area in Fig. 1) but also on its orientation. In three-point bending, σ and I are generally connected via $\sigma = F{\cdot}L{\cdot}h/(8\,I)$, [1]. The comparison with Eq. (1) yields $I = w{\cdot}h^3/12$ for the specimen in Fig. 1. Such moments have been calculated and are available for a number of cross sections, including rectangles, triangles, circles and many other shapes [2].

A relatively new trend in materials research is to combine nanoparticles with exceptional mechanical properties into macroscopic geometries by linking them with a second (organic) phase in a self-assembly process (see references [3–5] for overviews). In a recent publication from our group [6] (supplemental material [7]), these nanoparticles were surface functionalized, meaning that they were coated with a monomolecular layer of organic ligands on the surface, enabling their arrangement in so-called supercrystalline structures. However, small bending bars of this self-assembly material, produced at the Massachusetts Institute of Technology (MIT) and the Hamburg University of Technology (TUHH), have cross sections that are neither quadratic nor circular (see Fig. 2a) [6,7]. These shapes develop automatically during the production process. Therefore, as an alternative, the more realistic "flower shape" (Fig. 2b) has been chosen, composed of four overlapping circles. Its area moment of inertia can be calculated analytically, as completed in the next chapter.

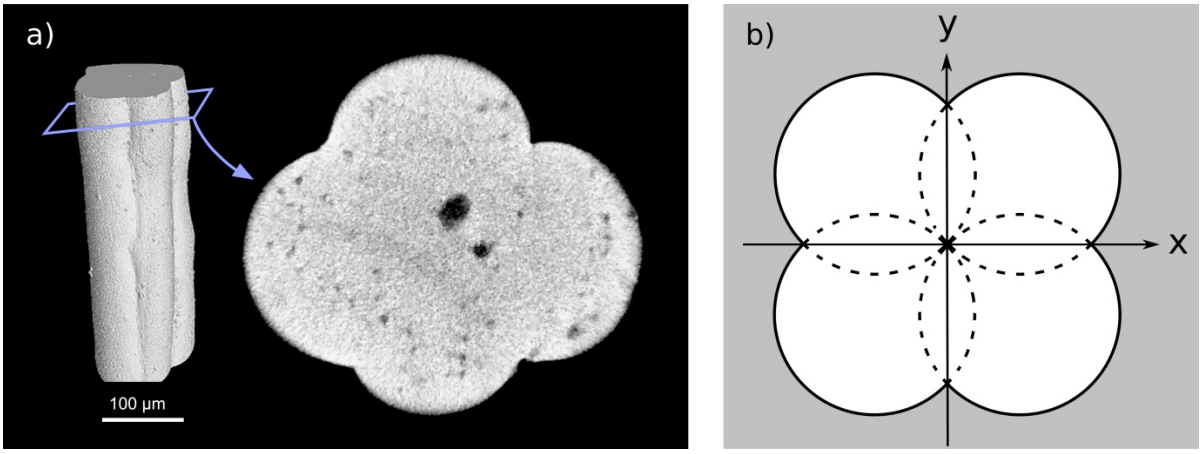

Fig. 2. a) Cross section of a self-assembly beam (prepared at the MIT, USA, 3D X-ray micrograph, recorded at the University of Bremen, Germany, and experiments performed at TUHH [6,7]). b) Mathematical shape in order to get a better estimate for the area moment of inertia. The opposing circles have point contact in the origin.

After finishing the calculation, the question arose of whether a rotation of the given shape around the origin changes the area moment of inertia. The answer led to two further generalizations concerning the influence of the rotation. At first, the result for the given fourfold symmetry was extended to the case of arbitrarily shaped cross sections with N-fold rotational symmetry for any $N \geq 3$. Secondly, the case of the area moment (second moment) of inertia was generalized to multipole moments of any order p. The corresponding equations were found for all combinations of N and p and the results show a complicated but well-ordered pattern, if they are arranged in an N-p matrix.

2. Calculation of Area Moment of Inertia

The area moment of inertia, also called the planar second moment of inertia, is defined by the following integral [1] over the area A

$$I_x = \iint_A y^2 \, \mathrm{d}A \qquad \text{or} \qquad I_y = \iint_A x^2 \, \mathrm{d}A \tag{2a,b}$$

where dA is the differential area in the cross section with the distance y or x from the reference plane. We use the second equation, implying that the intersection of the cross section and reference plane is the y-axis. First, we restrict the calculation to the upper right quadrant in Fig. 2b. Figure 3 represents this quadrant, where the radius of the circle is given by r and the measured "radius" of the sample by R. The center of the circle in Fig. 3 is placed at $(x, y) = (r/\sqrt{2}, r/\sqrt{2})$, implying that the equation for the circle is given by:

$$\left(x - \frac{r}{\sqrt{2}}\right)^2 + \left(y - \frac{r}{\sqrt{2}}\right)^2 = r^2 \tag{3}$$

Solving for y means:

$$y = \frac{r}{\sqrt{2}} \pm \sqrt{r^2 - \left(x - \frac{r}{\sqrt{2}}\right)^2} = \frac{r}{\sqrt{2}} \pm \sqrt{-x^2 + \sqrt{2}\, rx + \frac{r^2}{2}} \tag{4}$$

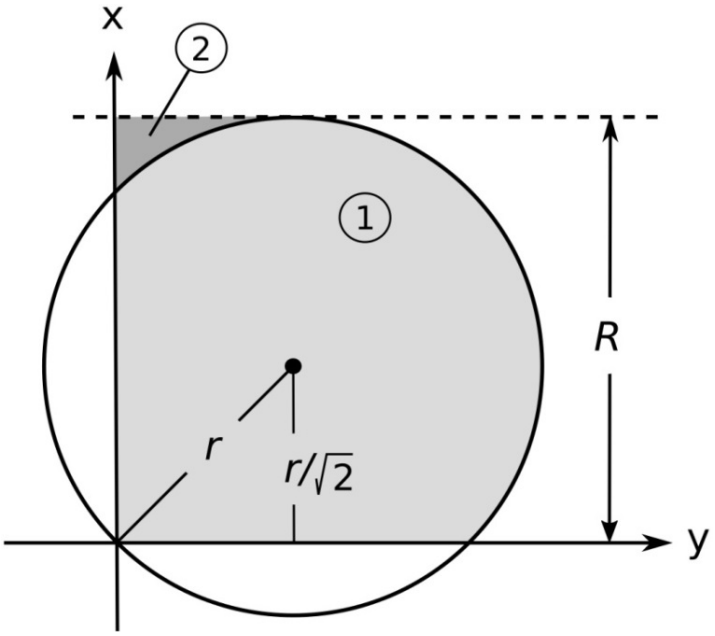

Fig. 3. Integration areas (1 and 2) for one quadrant. The area is weighted by x^2. The circle radius is r and the "sample radius" R. Note that the x- and y-axes are interchanged for presentation purposes, which does not change the calculation.

First, we integrate the combination of areas 1 and 2, yielding $I_{y(1,2)}$, and then subtract the integral of area 2, named $I_{y(2)}$. Hence, the area moment of inertia of one quadrant (Fig. 3) is given by

$$I_y = I_{y(1,2)} - I_{y(2)}$$

$$= \int_0^{r\left(1+\frac{1}{\sqrt{2}}\right)} \int_0^{\frac{r}{\sqrt{2}}+\sqrt{-x^2+\sqrt{2}\,rx+\frac{r^2}{2}}} x^2 \,\mathrm{d}y\,\mathrm{d}x - \int_{\sqrt{2}\,r}^{r\left(1+\frac{1}{\sqrt{2}}\right)} \int_0^{\frac{r}{\sqrt{2}}-\sqrt{-x^2+\sqrt{2}\,rx+\frac{r^2}{2}}} x^2 \,\mathrm{d}y\,\mathrm{d}x \qquad (5)$$

Note the different algebraic signs in the circle functions, which are used as upper integration limits. We start with the first integral $I_{y(1,2)}$. The y-integration is relatively simple. We obtain

$$I_{y(1,2)} = \int_0^{r\left(1+\frac{1}{\sqrt{2}}\right)} \left(\frac{r}{\sqrt{2}} + \sqrt{-x^2+\sqrt{2}\,rx+r^2/2}\right) \cdot x^2 \,\mathrm{d}x$$

$$= \int_0^{r\left(1+\frac{1}{\sqrt{2}}\right)} \frac{r}{\sqrt{2}}\, x^2 \,\mathrm{d}x + \int_0^{r\left(1+\frac{1}{\sqrt{2}}\right)} \sqrt{-x^2+\sqrt{2}\,rx+r^2/2} \cdot x^2 \,\mathrm{d}x \qquad (6)$$

(J_1) (J_2)

The two integrals in Eq. (6) are named J_1 and J_2. We find

$$J_1 = \frac{r}{\sqrt{2}} \frac{r^3\left(1+1/\sqrt{2}\right)^3}{3} = \frac{\left(1+1/\sqrt{2}\right)^3}{3\sqrt{2}} \cdot r^4 \qquad (7)$$

The "radius" R in Fig. 3 and the four quadrants are taken into account below. Solving the second integral J_2 in Eq. (6) is more complicated. The work of Bronstein and Semendjajew [8] provides the following integral, where a, b and c are constants with $a<0$ and $4ac-b^2<0$.

$$\int x^2 \sqrt{ax^2+bx+c}\ \mathrm{d}x \;=\; \left(x-\frac{5b}{6a}\right)\cdot\frac{(ax^2+bx+c)^{3/2}}{4a} \;+\; \frac{5b^2-4ac}{16\,a^2}\cdot$$

$$\cdot\left\{\frac{(2ax+b)\sqrt{ax^2+bx+c}}{4a}+\frac{4ac-b^2}{8a}\cdot\frac{-1}{\sqrt{-a}}\arcsin\frac{2ax+b}{\sqrt{b^2-4ac}}\right\} \qquad (8)$$

Comparison of this formula with the second integral J_2 in Eq. (6) yields

$$a=-1, \qquad b=\sqrt{2}\,r \qquad \text{and} \qquad c=\frac{r^2}{2} \qquad (9\text{a–c})$$

By replacing a, b and c in Eq. (8) with regard to Eqs. (9a–c) and by omitting the upper and lower bounds of the integral J_2, we find

$$\int \sqrt{-x^2+\sqrt{2}\,rx+r^2/2}\cdot x^2\,dx \;=\; \left(x+\frac{5\sqrt{2}\,r}{6}\right)\cdot\frac{\left(-x^2+\sqrt{2}\,rx+\frac{r^2}{2}\right)^{3/2}}{-4}$$

$$+\;\frac{3r^2}{4}\left\{\frac{\left(-2x+\sqrt{2}\,r\right)\sqrt{-x^2+\sqrt{2}\,rx+r^2/2}}{-4}\;-\;\frac{r^2}{2}\cdot\arcsin\left(\frac{-2x+\sqrt{2}\,r}{2r}\right)\right\} \qquad (10)$$

The calculation is standard but due to its complexity, mistakes can be made. Therefore, the next step is given in detail. Insertion of the integration limits leads to

$$J_2 \;=\; \int_0^{r\left(1+\frac{1}{\sqrt{2}}\right)} \sqrt{-x^2+\sqrt{2}\,rx+r^2/2}\cdot x^2\,\mathrm{d}x$$

$$=\;\left(r\left(1+\frac{1}{\sqrt{2}}\right)+\frac{5\sqrt{2}\,r}{6}\right)\frac{1}{-4}\left(-r^2\left(1+\frac{1}{\sqrt{2}}\right)^2+\sqrt{2}\,r^2\left(1+\frac{1}{\sqrt{2}}\right)+\frac{r^2}{2}\right)^{3/2}$$

$$+\;\frac{3r^2}{4}\left\{\frac{1}{-4}\left(-2r\left(1+\frac{1}{\sqrt{2}}\right)+\sqrt{2}\,r\right)\cdot\left(-r^2\left(1+\frac{1}{\sqrt{2}}\right)^2+\sqrt{2}\,r^2\left(1+\frac{1}{\sqrt{2}}\right)+\frac{r^2}{2}\right)^{1/2}\right.$$

$$\left.-\;\frac{r^2}{2}\cdot\arcsin\left(\frac{-2r\left(1+\frac{1}{\sqrt{2}}\right)+\sqrt{2}\,r}{2r}\right)\right\}$$

$$-\;\left(\frac{5\sqrt{2}\,r}{6}\left(\frac{r^2}{2}\right)^{3/2}\frac{1}{-4}+\frac{3r^2}{4}\left\{\frac{\sqrt{2}\,r\sqrt{\frac{r^2}{2}}}{-4}-\frac{r^2}{2}\arcsin\left(\frac{1}{\sqrt{2}}\right)\right\}\right) \qquad (11)$$

Reduction of this equation yields

$$J_2 \;=\; \left(\frac{3\pi}{16} - \left(-\frac{5}{48} - \frac{3}{16} - \frac{3\pi}{32}\right)\right) \cdot r^4 \;=\; \left(\frac{9\pi}{32} + \frac{7}{24}\right) \cdot r^4 \tag{12}$$

Note that the term $3\pi/16$ corresponds to the upper bound in Eq. (11). We will use this later. By adding J_1 and J_2 from Eqs. (7) and (12), the preliminary result is

$$I_{y(1,2)} \;=\; J_1 + J_2 \;=\; \left(\frac{\left(1 + 1/\sqrt{2}\right)^3}{3\sqrt{2}} + \frac{9\pi}{32} + \frac{7}{24}\right) \cdot r^4 \;=\; \left(\frac{10\sqrt{2} + 21}{24} + \frac{9\pi}{32}\right) \cdot r^4 \tag{13}$$

Next, the integral $I_{y(2)}$ from Eq. (5) is calculated. Its influence is not negligible because the distance of area 2 from the reference plane (y-axis) is relatively large. For this calculation, only the integration limits of $I_{y(1,2)}$ have to be replaced. As previously stated, we need the negative sign in front of the large square root in Eq. (4). Therefore, we obtain

$$\begin{aligned} I_{y(2)} \;&=\; \int_{\sqrt{2}\,r}^{r\left(1+\frac{1}{\sqrt{2}}\right)} \int_0^{\frac{r}{\sqrt{2}} - \sqrt{-x^2 + \sqrt{2}\,rx + \frac{r^2}{2}}} x^2 \,\mathrm{d}y \,\mathrm{d}x \\ &=\; \int_{\sqrt{2}\,r}^{r\left(1+\frac{1}{\sqrt{2}}\right)} \left(\frac{r}{\sqrt{2}} - \sqrt{-x^2 + \sqrt{2}\,rx + r^2/2}\right) \cdot x^2 \,\mathrm{d}x \\ &=\; \underbrace{\int_{\sqrt{2}\,r}^{r\left(1+\frac{1}{\sqrt{2}}\right)} \frac{r}{\sqrt{2}}\, x^2 \,\mathrm{d}x}_{(J_3)} \;-\; \underbrace{\int_{\sqrt{2}\,r}^{r\left(1+\frac{1}{\sqrt{2}}\right)} \sqrt{-x^2 + \sqrt{2}\,rx + r^2/2} \cdot x^2 \,\mathrm{d}x}_{(J_4)} \end{aligned} \tag{14}$$

The first integral is

$$J_3 \;=\; \frac{r}{\sqrt{2}} \left(\frac{r^3\left(1 + 1/\sqrt{2}\right)^3}{3} - \frac{\left(\sqrt{2}\,r\right)^3}{3}\right) \;=\; \frac{5\sqrt{2} - 1}{12} \cdot r^4 \tag{15}$$

The upper bound of J_4 has already been evaluated (see Eq. (12)). With $3\pi/16$, it follows

$$\begin{aligned} J_4 \;&=\; \frac{3\pi}{16} - \left(\sqrt{2}\,r + \frac{5\sqrt{2}\,r}{6}\right) \cdot \frac{\left(-2r^2 + 2r^2 + \frac{r^2}{2}\right)^{3/2}}{-4} \\ &\quad - \frac{3r^2}{4} \cdot \left\{\frac{\left(-2\sqrt{2}\,r + \sqrt{2}\,r\right) r/\sqrt{2}}{-4} - \frac{r^2}{2} \cdot \arcsin\left(\frac{-2\sqrt{2}\,r + \sqrt{2}\,r}{2r}\right)\right\} \\ &=\; \left(\frac{3\pi}{32} + \frac{1}{24}\right) \cdot r^4 \end{aligned} \tag{16}$$

Subtraction of J_4 from J_3 yields the integral of area 2 in Fig. 3.

$$I_{y(2)} \;=\; J_3 - J_4 \;=\; \left(\frac{5\sqrt{2} - 1}{12} - \frac{3\pi}{32} - \frac{1}{24}\right) \cdot r^4 \tag{17}$$

It follows for one quadrant:

$$I_y = I_{y(1,2)} - I_{y(2)} = \left(\frac{10\sqrt{2}+21}{24} + \frac{9\pi}{32} - \left(\frac{5\sqrt{2}-1}{12} - \frac{3\pi}{32} - \frac{1}{24} \right) \right) \cdot r^4 \qquad (18)$$

$$\Leftrightarrow \quad I_y = \left(\frac{3\pi}{8} + 1 \right) \cdot r^4 \qquad (19)$$

In order to use the sample radius R instead of r, we replace r by $R\sqrt{2}/(1+\sqrt{2})$. Furthermore, the moment of inertia is multiplied by 4 because of the four quadrants (Fig. 2b). Thus, we obtain the final result

$$I_y = \frac{2\,(3\pi+8)}{\left(1+\sqrt{2}\right)^4} \cdot R^4 = 1.0259 \cdot R^4 \qquad (20)$$

To confirm this result, an additional check is made. The same moment of inertia I_y is calculated by dividing the cross section (Fig. 3) into two alternative sections 3 and 4, as in Fig. 4.

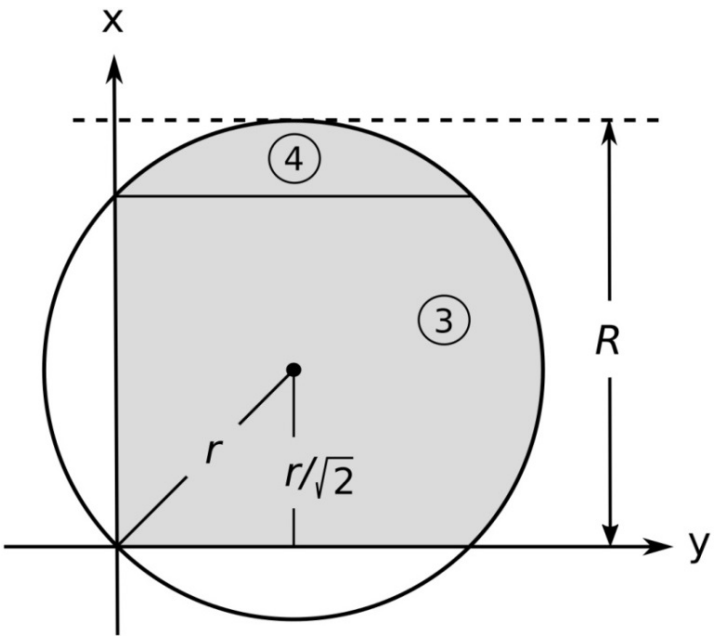

Fig. 4. Alternative segmentation of integration area.

We skip the detailed calculation steps. The results for the quadrant in Fig. 4 are

$$I_{y(3)} = \int_0^{\sqrt{2}\,r} \int_0^{\frac{r}{\sqrt{2}} + \sqrt{-x^2+\sqrt{2}\,rx+\frac{r^2}{2}}} x^2 \,\mathrm{d}y\,\mathrm{d}x = \left(\frac{3\pi}{16} + \frac{11}{12}\right) \cdot r^4 \qquad (21)$$

and

$$I_{y(4)} = \int_{\sqrt{2}\,r}^{r\left(1+\frac{1}{\sqrt{2}}\right)} \int_{\frac{r}{\sqrt{2}} - \sqrt{-x^2+\sqrt{2}\,rx+\frac{r^2}{2}}}^{\frac{r}{\sqrt{2}} + \sqrt{-x^2+\sqrt{2}\,rx+\frac{r^2}{2}}} x^2 \,\mathrm{d}y\,\mathrm{d}x = \left(\frac{3\pi}{16} + \frac{1}{12}\right) \cdot r^4 \qquad (22)$$

The sum of both quantities is exactly the result in Eq. (19).

3. Rotation of Cross Section

The cross sections of the micropillars do not always have the shape and orientation as presented in Fig. 2b but are sometimes twisted or distorted in another way. As a test, the cross section is rotated by 45° (Fig. 5) and the area moment of inertia with respect to the y-axis is calculated again. As before, we only consider the upper right quadrant which is divided into sections 5–7.

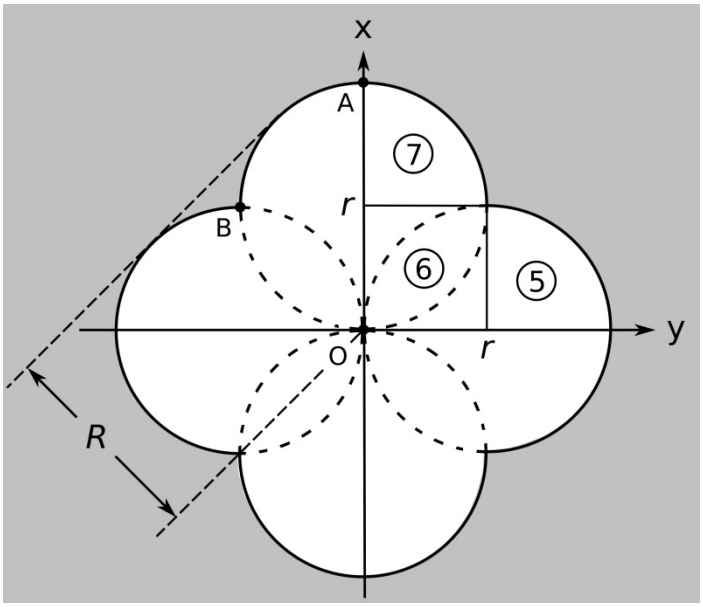

Fig. 5. Cross section rotated by 45° and division of the upper-right quadrant into areas 5, 6 and 7. Once more, the x- and y-axes are interchanged.

In this case, the calculation is easier because standard equations can be used for section 5 and for the quadratic area 6. We obtain [2]

$$I_{y(5)} = \frac{\pi}{16}\, r^4 \tag{23}$$

$$I_{y(6)} = \frac{1}{3}\, r^4 \tag{24}$$

For area 7, we determine the equation of the corresponding circle:

$$(x-r)^2 + y^2 = r^2$$

$$\Leftrightarrow \qquad y = \pm\sqrt{r^2-(x-r)^2} = \pm\sqrt{-x^2+2rx} \tag{25}$$

With the positive sign in front of the square root, it follows that

$$I_{y(7)} = \int_r^{2r}\int_0^{\sqrt{-x^2+2rx}} x^2\,\mathrm{d}y\,\mathrm{d}x = \int_r^{2r}\sqrt{-x^2+2rx}\;x^2\,\mathrm{d}x \tag{26}$$

Comparison with Eq. (8) yields

$$a = -1, \qquad b = 2\,r \qquad \text{and} \qquad c = 0 \tag{27a–c}$$

If we omit the integration bounds, we obtain

$$\int \sqrt{-x^2+2rx}\cdot x^2\,\mathrm{d}x \;=\; \left(x+\frac{5r}{3}\right)\cdot\frac{(-x^2+2rx)^{3/2}}{-4} \;+ \\ +\;\frac{5r^2}{4}\cdot\left\{\frac{(-2x+2r)\sqrt{-x^2+2rx}}{-4}-\frac{r^2}{2}\cdot\arcsin\frac{-2x+2r}{2r}\right\} \tag{28}$$

After inserting the bounds of integration and reducing the mathematical term, we find

$$I_{y(7)} \;=\; \int_r^{2r}\sqrt{-x^2+2rx}\;x^2\,\mathrm{d}x \;=\; \left(\frac{5\pi}{16}+\frac{2}{3}\right)\cdot r^4 \tag{29}$$

Adding the contributions of the three sections in Fig. 5 results in

$$I_y \;=\; I_{y(5)}+I_{y(6)}+I_{y(7)} \\ =\;\left(\frac{\pi}{16}+\frac{1}{3}+\frac{5\pi}{16}+\frac{2}{3}\right)\cdot r^4 \;=\; \left(\frac{3\pi}{8}+1\right)\cdot r^4 \tag{30}$$

This is the same outcome that we have in Eq. (19). Actually, this identity is not accidental. Let us assume that the reference axis "η" has been rotated by an angle α. Then, the following equation is valid [2]

$$I_\eta(\alpha) \;=\; \sin^2\alpha\iint y^2\mathrm{d}A \;+\; \cos^2\alpha\iint x^2\mathrm{d}A \;-2\sin\alpha\cos\alpha\iint yx\,\mathrm{d}A \tag{31}$$

The rotation angle α is measured from the x-axis. In our case in Fig. 2b, the cross section is identical after rotation by 90°, implying $I_x = I_y = I$. The first and second integrals in Eq. (31) are I_x and I_y, respectively, and the third integral vanishes because of symmetry reasons. Hence, Eq. (31) becomes

$$I_\eta(\alpha) \;=\; \sin^2\alpha\cdot I+\cos^2\alpha\cdot I \;=\; I \tag{32}$$

This means that the area moment of inertia of the cross section in Fig. 2b is not only unchanged after rotating by 45°, but it remains constant for any rotation angle. Furthermore, this holds for any cross section, which is identical after the 90° rotation, like for a square. Note that these shapes do not necessarily have axial symmetry with respect to an axis in the xy-plane.

The contour of the "flower-shaped" cross section has different radii, dependent on where they are measured. Let the origin in Fig. 5 be named "O", then the maximum radius (AO) is $2r$ and the minimum radius (BO) is $\sqrt{2}r$ (see Fig. 5). Interestingly, the arithmetic mean $(2r+\sqrt{2}r)/2$ of both radii is equal to R, as defined in Figs. 3–5.

4. Some Physical Quantities

Table 1 summarizes the equations of the area moment of inertia I, Young's modulus E, stress σ and strain ε (compare Ref. [9]) for the quadratic, circular and "flower-shaped" cross

sections. For better comparability, the edge length of the square is labeled $2R$. By including also the rotation (α), we have to be careful when defining the relevant height of the sample. Thus, we introduce the "radius" R' in Fig. 6, which is half of the height h (compare Fig. 1). Therefore, if the cross section is rotated by α, the maximum stress and strain depend proportionately on R', whereas I and E are independent of R' (and α). The results are based on linear elastic material behavior.

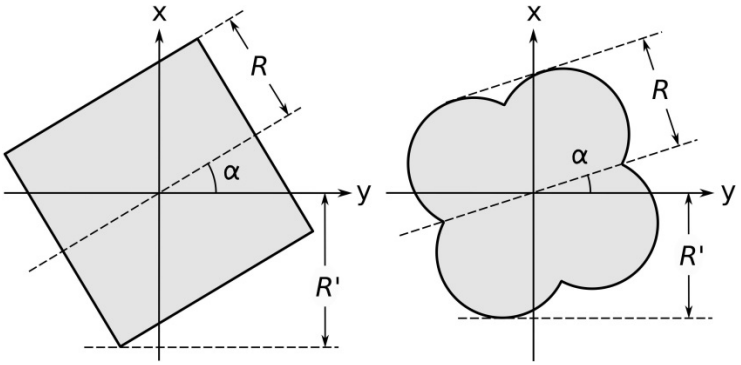

Fig. 6. Illustrations of R and R'. R defines the size of the cross section and R' specifies half of the height with respect to the x- or y-axis.

Table 1. Various physical quantities for three-point bending measurements for three different cross sections, including the case of a rotation by an arbitrary angle. L is the support distance, F and d are force and displacement at the central load point, respectively, and s ($=F/d$) is the slope in the F-d-diagram. The beam radii R and R' with $2R' = h$ are defined as in Fig. 6. Stress and strain refer to the outer fiber at the center of the beam. These quantities are connected via $\sigma = F \cdot L \cdot R'/(4I)$ and $E = \sigma/\varepsilon$. For the circle, we use only R because of $R' = R$.

Cross section			
Area moment of inertia I	$\frac{4}{3} \cdot R^4$ $= 1.3333 \cdot R^4$	$\frac{\pi}{4} \cdot R^4$ $= 0.7854 \cdot R^4$	$\frac{2\,(3\pi + 8)}{\left(1+\sqrt{2}\right)^4} \cdot R^4$ $= 1.0259 \cdot R^4$
Young's modulus E	$\frac{L^3 s}{64\,R^4}$ $= 0.015625 \cdot \frac{L^3 s}{R^4}$	$\frac{L^3 s}{12\,\pi\,R^4}$ $= 0.026526 \cdot \frac{L^3 s}{R^4}$	$\frac{\left(1+\sqrt{2}\right)^4 L^3 s}{96\,(3\pi + 8)\,R^4}$ $= 0.020308 \cdot \frac{L^3 s}{R^4}$
Stress σ (strength)	$\frac{3\,F\,L\,R'}{16\,R^4}$ $= 0.18750 \cdot \frac{F\,L\,R'}{R^4}$	$\frac{F\,L}{\pi\,R^3}$ $= 0.31831 \cdot \frac{F\,L}{R^3}$	$\frac{\left(1+\sqrt{2}\right)^4 F\,L\,R'}{8\,(3\pi + 8)\,R^4}$ $= 0.24369 \cdot \frac{F\,L\,R'}{R^4}$
Strain ε	$\frac{12\,d\,R'}{L^2}$	$\frac{12\,d\,R}{L^2}$	$\frac{12\,d\,R'}{L^2}$

If the square or the flower shape are aligned parallel to the x- and y-axes (like in Fig. 2b), we have $R' = R$. Thus, concerning the square in Table 1, the expression for stress is reduced to $3FL/(16\,R^3)$. The term of stress for the flower-shaped cross section is simplified accordingly. It should be noted that R' is linked to α via the shape of the cross section.

5. *N*-fold Rotational Symmetry

It has been shown that the area moment of inertia of a cross section with fourfold rotational symmetry does not depend on the orientation (α) of the cross section. The question is whether this is valid also for threefold, fivefold or any N-fold rotational symmetry. An example of an area with threefold symmetry is given by the rotor shape of a wind energy converter (Fig. 7).

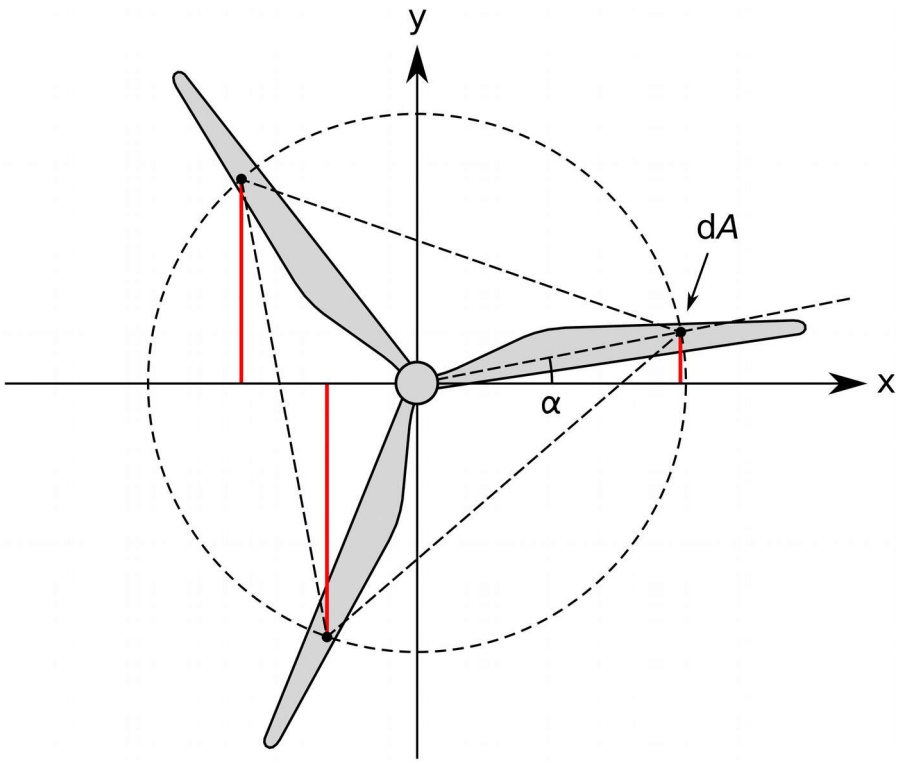

Fig. 7. Rotor with threefold rotational symmetry. It is composed of small areas dA, which can be arranged in equilateral triangles. The distances in red are relevant for the area moment of inertia.

In order to check the independence from the angle α, we assume an infinitesimal area dA somewhere on one of the three rotor blades, represented by a black dot in Fig. 7. The desired physical quantity of each blade (area moment of inertia) can be obtained by integration along such small areas dA over the whole (two-dimensional) surface of one blade. A rotation by 120° moves this point to the next blade in the corresponding position and another 120° rotation to the third blade. The three black dots build an equilateral triangle. The main idea is that we supply each of the three points with a "unit mass" 1 (unit area 1), rotate only this triple by α and check whether the area moment of inertia of these combined points has changed or not. If not, the result is valid also for the whole rotor, because the latter is completely composed of such "mass triples", arranged in equilateral triangles. Moreover, the same argument is valid for any regular polygon and realistic cross section with N-fold rotational symmetry.

The shape of the rotor is definitely not typical for the cross section of a bending bar, it is just used to illustrate the principle. Note that the reference axis for the calculation of the moment of inertia is not the rotation axis of the rotor but the x-axis (or the y-axis). Without limiting the generality, we will further focus on "mass points" confined to the unit circle. Thus, the red lines in Fig. 7 are the sine values of the corresponding angles. Next, we assume N points with equidistant positions on the unit circle, which includes the case $N=3$ in Fig. 7. The related area moment of inertia, I_x, is given by

$$I_x = \sum_{k=1}^{N} \sin^2\left(\alpha + \frac{2\pi k}{N}\right) \tag{33}$$

which refers to the x-axis and is valid for N equally distributed points on the unit circle, each with a "mass" of 1 and a "phase shift" α. Actually, instead of $k=1\ldots N$, the range $k=0\ldots N-1$ would be compliant with Fig. 7, however, both index ranges yield the same result. In order to calculate the sum, we use the identity $\sin^2 x = {}^1/_2 \cdot (1-\cos(2x))$ and obtain

$$I_x = \sum_{k=1}^{N} \frac{1}{2}\left(1-\cos\left(2\alpha + \frac{4\pi k}{N}\right)\right) \tag{34}$$

By applying $\cos(x+y) = \cos x \cdot \cos y - \sin x \cdot \sin y$, we find

$$\begin{aligned} I_x &= \sum_{k=1}^{N} \frac{1}{2}\left(1 - \left(\cos(2\alpha)\cdot\cos\frac{4\pi k}{N} - \sin(2\alpha)\cdot\sin\frac{4\pi k}{N}\right)\right) \\ &= \frac{N}{2} - \frac{\cos(2\alpha)}{2}\cdot\sum_{k=1}^{N}\left(\cos\frac{4\pi k}{N}\right) + \frac{\sin(2\alpha)}{2}\cdot\sum_{k=1}^{N}\left(\sin\frac{4\pi k}{N}\right) \end{aligned} \tag{35}$$

In order to evaluate both summations, we use two equations from J. L. Lagrange [10]:

$$\sum_{k=1}^{N} \sin(k\theta) = \frac{1}{2}\cot\frac{\theta}{2} - \frac{\cos((N+1/2)\theta)}{2\sin(\theta/2)} \tag{36}$$

and

$$\sum_{k=1}^{N} \cos(k\theta) = -\frac{1}{2} + \frac{\sin((N+1/2)\theta)}{2\sin(\theta/2)} \tag{37}$$

The comparison of the last sum in Eq. (35) with the sum in Eq. (36) yields $\theta = 4\pi/N$, equivalent to $N\theta = 4\pi$. Therefore, we have a summand 4π in the argument of the cosine function in Eq. (36) and can skip this double round angle. The numerator becomes $\cos(\theta/2)$ and it can be seen that the right side of Eq. (36) vanishes. With the same argumentation, also the right side of Eq. (37) becomes zero. This means that the summations in Eq. (35) both disappear and we are left with the result:

$$I_x = \frac{N}{2} \tag{38}$$

It follows that the area moment of inertia is independent of α for any number (≥ 3) of equally distributed points on a circle. It depends only on the number of points N. The same independence is valid for realistic cross sections of any shape with N-fold axial symmetry and $N \geq 3$.

Equation (38) belongs to the (also named) planar second moment of inertia. Concerning the two sums in Eq. (35), they can be related to the "first moment" or moment of force (torque). Now, it can easily be shown that, after including a constant angle (α), which enters the cosine or sine argument in the sums of Eq. (35), the result is unchanged. The calculation, which is omitted here, is analog to the step from Eq. (34) to Eq. (35). Hence, the main differences between the last sum in Eq. (35) and the sum in Eq. (33) are the exponent 1 instead of 2 and the factor 4π instead of 2π. Concerning 4π, we find that if N is even and $N \geq 4$, only the number of points on the unit circle is reduced from N to $N/2$. For odd $N \geq 3$, the number of points remains the same, just the sequence of the points, if numbered from 1 to N, varies. Hence, we can replace the two factors 4π in Eq. (35) each by 2π and add α. Then, the last sum in Eq. (35) corresponds exactly to the moment of force (for N points of mass 1 on the unit circle). It follows that this moment is always zero. In Fig. 8, the situation is shown for a hexagon and a pentagon.

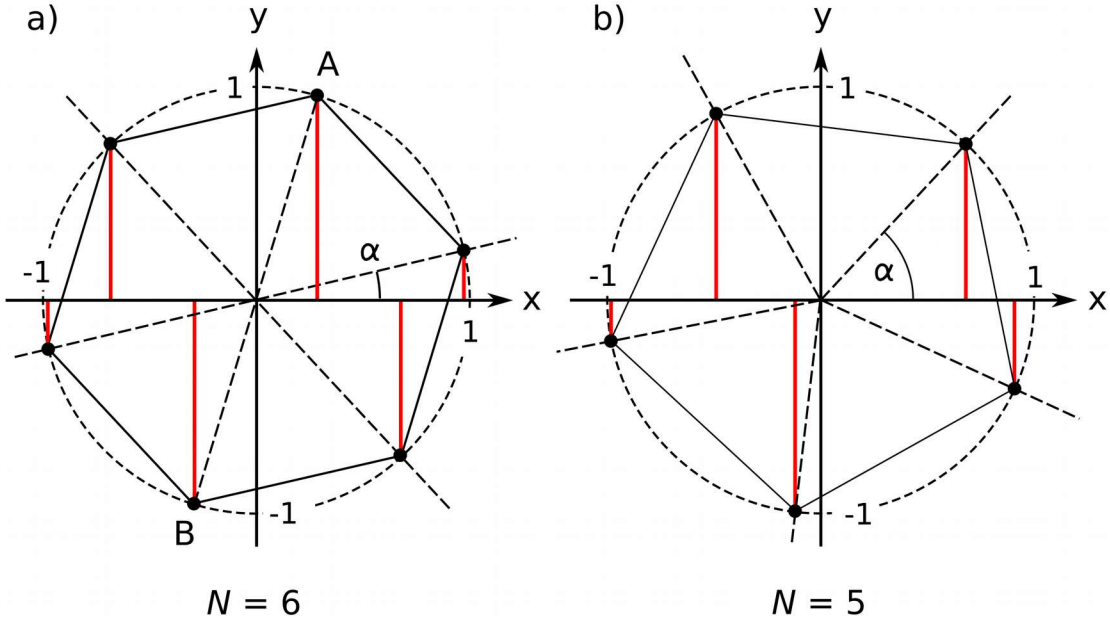

Fig. 8. Equally distributed mass points on the unit circle with a) sixfold and b) fivefold rotational symmetry.

For the hexagon, the result is obvious. With respect to the moment of force, each two opposing points, like A and B, cancel each other, because of point symmetry and different algebraic signs. For the pentagon, this argument does not work. But also here, a simple reason explains why the resulting moment is zero. Due to the regularity of the pentagon, the center of mass of the five points is located in the origin, which is placed on the x-axis. A rotation by any angle α does not change the situation. Therefore, the center of mass on the reference axis (x-axis) always means zero moment, which is valid for any $N \geq 2$.

6. Multipole Moments of Higher Order

The first and second moments of any realistic shape with rotational symmetry are independent of the rotation angle α. For N unit masses on the unit circle with the corresponding symmetry, the first moment is always zero for $N \geq 2$ and the second moment is $N/2$ for $N \geq 3$.

The question comes up if similar equations exist for multipole moments of higher order (higher power than 2 in Eq. (33)) and if the results are always independent of α? Indeed, results independent of α can be obtained for any high order p, but for certain combinations of N and p, the results depend on α. Before we continue, a brief overview of moments is given in Table 2.

Table 2. A summary of moments of different orders in physics and mathematics. Other multipole moments, e.g., related to electric, magnetic or gravitational fields, are not included here.

Order p of moment	**Mechanics**	**Statistics**
0 (zeroth moment)	Total mass	Total probability (=1)
1 (first moment)	Moment, center of mass	Expected value
2 (second moment)	Area (mass) moment of inertia	Central moment (variance)
3 (third moment)	—	Skewness of distribution
4 (fourth moment)	—	Kurtosis of distribution
$p \geq 5$	—	Sample moments

For the sake of completeness, the zeroth moment is included in Table 2. If the exponent 2 in Eq. (33) is replaced by 0, the result becomes N, which is the total mass because each point has the mass 1. Actually, fixing the masses to 1 and the positions to the unit circle is carried out because it simplifies the equations, but it does not restrict the main results. The "center of mass" in Table 2 refers to its position (distance to the reference axis), which is obtained after dividing the outcome by the total mass.

The following generalization to multipole moments is not so relevant in mechanics, but it is relevant in mathematics and it reveals some interesting results. In order to have an overview, a simple Fortran program was written, using Eq. (33) with the exponent p instead of 2, and the results were calculated and checked step by step. (Of course, this can be achieved with any other programming language, too.) The input parameters N (number of points) and p (exponent of the sine function) are natural numbers and the angle α can be any real number.

The results are compiled in Table 3. The abbreviation "var." (marked in gray) means that these moments are "variable", because they depend on α. It does not mean "not defined" because the moments can be calculated for any α. The simplest cases are the results for odd exponents p. According to Fig. 8b, perhaps, we would expect that these results are always zero, because odd p means plus and minus signs in the summation. However, the summands cancel each other for $N > p$, but not in every case for $N \leq p$.

Next, we examine the moments for even exponents p. Naturally, all the results are positive. Nevertheless, also here, not all of them are independent of α. But first, we will search for an equation that is universally valid for any even p and any $N > p$.

If we take the denominators of the fractions in Table 3 for the even exponents p = 2, 4, 6, ..., we have 2, 8, 32, 128, 512, ... It is obvious that these numbers are given by 2^{p-1}. In contrast, the sequence of the numerators is not that simple. For the same sequence of even p and by

Table 3. Calculated multipole moments, based on Eq. (33) with the exponent 2 replaced by p. The moments depend on p, on the number of points N and partly on α. "Var." stands for "variable". The meaning of the asterisk (*) is described further below. The white fields indicate the results that are independent of α. Fixed positive numbers can be found only to the right of the red line. The blue field at $N=2$ and $p=2$ belongs to standard bending bars (rectangular cross sections). The second blue field at $N=4$ and $p=2$ refers to the flower-shaped cross section in Figs. 2b and 5 and to the square. The fractions are not reduced so that the principles can be better seen.

	$N=1$	2	3	4	5	6	7	8	9	10	11	12	13
$p=1$	var.	0	0	0	0	0	0	0	0	0	0	0	0
2	var.	var.	$\frac{3}{2}$	$\frac{4}{2}$	$\frac{5}{2}$	$\frac{6}{2}$	$\frac{7}{2}$	$\frac{N}{2}$	$\rightarrow$				
3	var.	0	var.	0	0	0	0	0	0	0	0	0	0
4	var.	var.	$\frac{9}{8}$	var.*	$\frac{15}{8}$	$\frac{18}{8}$	$\frac{21}{8}$	$\frac{24}{8}$	$\frac{3N}{8}$	$\rightarrow$			
5	var.	0	var.	0	var.	0	0	0	0	0	0	0	0
6	var.	var.	var.	var.*	$\frac{50}{32}$	var.	$\frac{70}{32}$	$\frac{80}{32}$	$\frac{90}{32}$	$\frac{10N}{32}$	$\rightarrow$		
7	var.	0	var.	0	var.	0	var.	0	0	0	0	0	0
8	var.	var.	var.	var.*	$\frac{175}{128}$	var.	$\frac{245}{128}$	var.*	$\frac{315}{128}$	$\frac{350}{128}$	$\frac{35N}{128}$	$\rightarrow$	
9	var.	0	var.	0	var.	0	var.	0	var.	0	0	0	0
10	var.	var.	var.	var.*	var.	var.	$\frac{882}{512}$	var.*	$\frac{1134}{512}$	var.	$\frac{1386}{512}$	$\frac{126N}{512}$	$\rightarrow$
11	var.	0	var.	0	var.	0	var.	0	var.	0	var.	0	0
12	var.	var.	var.	var.*	var.	var.	$\frac{3234}{2048}$	var.*	$\frac{4158}{2048}$	var.	$\frac{5082}{2048}$	var.*	$\frac{462N}{2048}$
13	var.	0	var.	0	var.	0	var.	0	var.	0	var.	0	var.
14	var.	var.	var.	var.*	var.	var.	var.	var.*	$\frac{15444}{8192}$	var.	$\frac{18876}{8192}$	var.*	$\frac{1716N}{8192}$

skipping the factor N, we obtain the numbers 1, 3, 10, 35, 126, etc. After some trial and error, the following expression was found, given on the left side of Eq. (39).

$$\prod_{k=2}^{p/2}\left(3+\sum_{j=2}^{k-1}\frac{2}{j(j+1)}\right) \quad = \quad \frac{1}{2}\cdot\binom{p}{\frac{p}{2}} \tag{39}$$

Later, it turned out that this combination of product and sum is equal to half of the (central) binomial coefficient on the right side of Eq. (39). Therefore, in principle, we don't need the complicated term on the left side. However, we keep Eq. (39) here as a mathematical curiosity.

Please note that if the upper bound of k in the multiple product is lower than the starting value, the product equals one. If the upper bound of j in the summation is lower than the starting value, the sum is zero. This is illustrated by the examples

$$\prod_{k=2}^{1} A_k \;=\; 1 \qquad \text{and} \qquad \sum_{j=2}^{1} A_j \;=\; 0 \;, \tag{40a,b}$$

where A_k and A_j can be any real terms. Without these conventions, the above cases would be treated in an extra way, and Eq. (39) would become more complicated. For a better understanding, an example is given. Both sides of Eq. (39) are calculated for the exponent $p = 10$.

$$\prod_{k=2}^{5}\left(3+\sum_{j=2}^{k-1}\frac{2}{j(j+1)}\right) \;=\; 3\cdot\left(3+\frac{2}{2\cdot3}\right)\cdot\left(3+\frac{2}{2\cdot3}+\frac{2}{3\cdot4}\right)\cdot\left(3+\frac{2}{2\cdot3}+\frac{2}{3\cdot4}+\frac{2}{4\cdot5}\right) \;=\; 126 \tag{41}$$

$$\frac{1}{2}\cdot\binom{10}{5} \;=\; \frac{1}{2}\cdot\frac{10\cdot9\cdot8\cdot7\cdot6}{1\cdot2\cdot3\cdot4\cdot5} \;=\; 126 \tag{42}$$

Equation (39) can be verified. In case, the reader is interested, he/she may try to prove Eq. (39). Otherwise, a proof is provided in the Appendix A.

In Table 3, we can identify three different areas. To the right of the diagonal ($N > p$), the solutions are positive or zero and always independent of α. Between this diagonal and the red polygon, given by $p/2 < N \le p$, we have positive and zero solutions, as well as cases dependent on α. The third area to the left of the red polygon only contains zeros and variable solutions. Since α can be any angle, we are allowed to change α to $\alpha + \pi/2$ and, because of $\sin(x+\pi/2) = \cos x$, we can replace the sine function, e.g., in Eq. (33), by the cosine function. Thus, by combining numerators and denominators (Table 3), we obtain the following three final cases a) – c) of multipole moments with $p \ge 1$ and $N \ge 1$.

a) If p is even and $N > p$ or if p is even, N odd and $p/2 < N < p$, then the following two equations hold, in which α can be any real number:

$$\sum_{k=1}^{N}\sin^p\left(\alpha+\frac{2\pi k}{N}\right) \;=\; \frac{N}{2^p}\binom{p}{\frac{p}{2}} \tag{43}$$

$$\sum_{k=1}^{N}\cos^p\left(\alpha+\frac{2\pi k}{N}\right) \;=\; \frac{N}{2^p}\binom{p}{\frac{p}{2}} \tag{44}$$

b) If p is odd and $N > p$ or if p is odd, N even and $N < p$, then we find for any real α:

$$\sum_{k=1}^{N}\sin^p\left(\alpha+\frac{2\pi k}{N}\right) \;=\; 0 \tag{45}$$

$$\sum_{k=1}^{N}\cos^p\left(\alpha+\frac{2\pi k}{N}\right) \;=\; 0 \tag{46}$$

c) In all other cases, the sum varies, dependent on α (see "var." in Table 3).

Table 3 was generated by numerical calculation and Eq. (43)–(46) were found empirically. Nevertheless, these equations could be verified and also the reason for their peculiar range of definition, as illustrated in Table 3, was found. The proof is provided in the Appendix B. For the general solution, including all of the "var."-positions of Table 3, see Appendix C.

It should be mentioned that Table 3 does not deliver solutions for the area moments of inertia of realistic cross sections such as, for example, Eq. (20). Those calculations still have to be completed. Moreover, for the simple case of mass points on the unit circle, as given here, the p^{th} moment can be obtained easily by numerical calculation, for instance, with the left side of Eq. (43). Anyway, the table shows what we can expect for certain parameters N and p, with special focus on the dependence on α. It is also interesting that we do not have a simple rule for all of the combinations of N and p but a relatively complex pattern.

7. Summary

The area moment of inertia of a "flower-shaped" cross section with fourfold rotational symmetry has been calculated analytically. It was also shown for cross sections with an N-fold rotational symmetry that this moment does not change if the cross section is rotated by an arbitrary angle. In case of moments of higher order, the constancy of the moment, with respect to a rotation, is not valid for certain combinations of the orders of symmetry and multipole moment. This is described by Eqs. (43)–(46) which could be verified, and also their unusual range of definition (concerning N and p) became plausible. An even better understanding of this phenomenon is possible on the basis of another complete set of equations ((C5)–(C8)).

Acknowledgments

We thank Dr. Berta Domènech and Prof. Dr. Lucio Colombi Ciacchi for providing and allowing the use of Fig. 2a and especially Dipl.-Phys. Oliver Focke for having created this image. We are indebted to Dr. Heinrich Streckwall (HSVA) for providing the main calculation steps which enabled the proof of Eqs. (43)–(46), and for the idea how to avoid the singularity which led to Eqs. (C1)–(C8). Furthermore, we thank Prof. Dr. Gerold A. Schneider for giving some valuable hints. This work was supported by the German Research Foundation (DFG), project number 192346071, SFB 986.

Appendix A. Proof of Eq. (39)

The proof is performed by induction, which shows that a statement S_n is valid for every natural number $n = 1, 2, 3, ...$ In Eq. (39), we replace the even number p by $2n$ and, thus, prove the following equivalent formula for every n. This verifies also Eq. (39).

$$\prod_{k=2}^{n} \left(3 + \sum_{j=2}^{k-1} \frac{2}{j(j+1)} \right) = \frac{1}{2} \cdot \binom{2n}{n} \tag{A1}$$

Base case

If we check the first three cases and insert n = 1, 2 and 3 into Eq. (A1), we obtain 1, 3 and 10 on both sides of the equation. For the left side, the results can be seen directly with Eqs. (41) and (40a,b). For the right side, the details can be easily confirmed on the basis of

$$\binom{2n}{n} \;=\; \frac{(2n)!}{n!\cdot(2n-n)!} \;=\; \frac{(2n)!}{(n!)^2} \tag{A2}$$

Induction step

We assume that Eq. (A1) is valid for n. Now, we can see that we get from n to the next case n+1 on both sides of Eq. (A1) by multiplication with a certain factor. On the left side, we name this factor B_{n+1}, which is given by the term in the large brackets. The index k in this factor would be $k = n+1$. Hence, the upper bound of the summation is $(n+1)-1 = n$, meaning

$$B_{n+1} \;=\; 3 + \sum_{j=2}^{n} \frac{2}{j(j+1)} \tag{A3}$$

In order to take the same step from n to n+1 on the right side of Eq. (A1), we have the following equation:

$$\frac{1}{2}\cdot\binom{2n}{n}\cdot\frac{(2n+2)\cdot(2n+1)}{(n+1)^2} \;=\; \frac{1}{2}\cdot\binom{2(n+1)}{n+1} \tag{A4}$$

The latter equation can be illustrated with the help of Eq. (42) by changing p (= 2n) from 10 to 12 and considering the additional factors. Thus, the respective factor on the right side of Eq. (A1), named C_{n+1}, is

$$C_{n+1} \;=\; \frac{(2n+2)\cdot(2n+1)}{(n+1)^2} \;=\; \frac{4n+2}{n+1} \tag{A5}$$

If we go, for example, from $n = 1$ to 2 in Eq. (A1), the corresponding factor is 3 and from $n = 2$ to 3, we have $3^1/_3$ (see also Eq. (41)). Next, we concentrate on the differences of two successive factors, which are defined by $\Delta B_{n+1} = B_{n+1} - B_n$ and $\Delta C_{n+1} = C_{n+1} - C_n$. If we can demonstrate $\Delta B_{n+1} = \Delta C_{n+1}$ for every n, then this would imply $B_{n+1} = C_{n+1}$ and Eq. (A1) would be valid for the case n+1. It would follow directly that Eqs. (A1) and (39) are generally correct.

The determination of ΔB_{n+1} and ΔC_{n+1} is simple. It turns out that ΔB_{n+1} is given by the last summand of the summation in Eq. (A3) – see also Eq. (41). This means

$$\Delta B_{n+1} \;=\; \frac{2}{n\cdot(n+1)} \tag{A6}$$

and according to Eq. (A5), we find

$$\Delta C_{n+1} \;=\; C_{n+1} - C_n \;=\; \frac{4n+2}{n+1} - \frac{4(n-1)+2}{n} \;=\; \frac{2}{n\cdot(n+1)}\;. \qquad \text{Q.E.D.} \tag{A7}$$

Remark: By taking into account that the sum of the natural numbers from 1 to j is equal to $j(j+1)/2$ and after rewriting Eq. (A1) accordingly, the central binomial coefficient satisfies the equation ($n \geq 1$):

$$\binom{2n}{n} \;=\; 2\cdot\prod_{k=2}^{n}\left(3+\sum_{j=2}^{k-1}\left(\sum_{i=1}^{j} i\right)^{-1}\right) \tag{A8}$$

This formula does not directly refer to the objective of this article, but it seems to be new and is kept as a byproduct.

Appendix B. Proof of Eqs. (43)–(46)

We have to prove only Eqs. (43) and (45) because, due to the variability of α, Eqs. (44) and (46) can be seen as being equivalent to the latter two equations. We start with Eq. (43), meaning that p is even. Based on Euler's formula, we obtain

$$\sin^p x \;=\; \left(\frac{e^{\mathrm{i}x}-e^{-\mathrm{i}x}}{2\mathrm{i}}\right)^p \tag{B1}$$

By using the binomial theorem and taking into account $\binom{p}{m}=\binom{p}{p-m}$, we find for even p [11]:

$$\sin^p x \;=\; \frac{1}{2^p}\binom{p}{\frac{p}{2}} + \frac{1}{2^{p-1}}\cdot\sum_{m=0}^{p/2-1}(-1)^{p/2-m}\binom{p}{m}\cos\big((p-2m)x\big) \tag{B2}$$

Temporarily, we omit α, replace x by $2\pi k/N$ and include the summation over k from Eq. (43). In addition, the sum over k is shifted into the sum over m. This means

$$\sum_{k=1}^{N}\sin^p\left(\frac{2\pi k}{N}\right) \;=\; \frac{N}{2^p}\binom{p}{\frac{p}{2}} + \frac{1}{2^{p-1}}\cdot\sum_{m=0}^{p/2-1}\left((-1)^{p/2-m}\binom{p}{m}\cdot\sum_{k=1}^{N}\cos\left((p-2m)\frac{2\pi k}{N}\right)\right) \tag{B3}$$

The latter modification is allowed because all of the factors in front of the sum over k are independent of k for each m-value. By applying the summation to the first term on the right side of Eq. (B2), this term becomes identical to the right side of Eq. (43). If applying again Lagrange's trigonometric identity (Eq. (37)), the summation over k on the right becomes

$$\sum_{k=1}^{N}\cos\left((p-2m)\frac{2\pi k}{N}\right) \;=\; -\frac{1}{2} + \frac{\sin\big((N+1/2)(p-2m)\cdot 2\pi/N\big)}{2\,\sin\big((p-2m)\cdot 2\pi/(2N)\big)} \tag{B4}$$

Now, we multiply N in the bracket (N+1/2) with the other factors in the numerator and obtain (p–2m)$\cdot 2\pi$, being an integer multiple of 2π. Therefore, we can omit this N in the sine argument and find

$$\sum_{k=1}^{N}\ldots \;=\; -\frac{1}{2} + \frac{\sin\big((1/2)(p-2m)\cdot 2\pi/N\big)}{2\cdot\sin\big((p-2m)\cdot 2\pi/(2N)\big)} \;=\; 0 \tag{B5}$$

being valid for even p and for any value of the summation index m (in case of $N>p$). Thus, the sum over m in Eq. (B3) vanishes and we get Eq. (43) but without the phase shift α. If we

include α and consider it in a similar way than the step from Eq. (34) to Eq. (35) as well as apply Lagrange's identity, the result (zero) remains unchanged. The calculation does not contain any further difficulty and proves Eqs. (43) and (44) within their range of definition.

However, these equations are not generally valid. If looking at the range $N \le p$ in Table 3, there are combinations of N and p where both equations do not work (see "var."). This is true even partly for the case $\alpha = 0$. The reason can be found in Eq. (B5). Numerator and denominator, containing the sine functions, must not be zero, which would be the case if the (identical) arguments vanish. Anyway, the factor $p - 2m$ in the arguments is always positive because the maximum value of m is $p/2 - 1$, and therefore, the arguments cannot be zero. On the other hand, the sine becomes zero as well if the argument is equal to a multiple of π, meaning π, 2π, 3π, etc. Since the arguments are $(p - 2m) \cdot \pi/N$, the factor $(p - 2m)/N$ must not be an integer. If checking this, it has to be taken into account that for given N and p, the summation index m has different values. For example, $p = 8$ means that m is successively equal to 0, 1, 2 and 3. If one of these cases yields an integer, the equation is not true because 0/0 is not defined.

In view of Table 3, it is obvious that for $N > p$, we always have $0 < (p - 2m)/N < 1$, implying that we cannot obtain an integer. With $N = 3$ and $p = 8$, on the other hand, the term becomes integer for $m = 1$, meaning that this case has to be excluded. By checking other cases in Table 3, it turns out that the given number $(p - 2m)/N$ with "p even" becomes integer for each position, referred to as "var.", and only for these positions. After all, it seems that the application of the Lagrange's identity in Eqs. (B4) and (B5) explains very well the whole pattern of valid and "var."-positions in Table 3 (for even p). Finally, the case of odd p is treated briefly.

Considering Eq. (45) and odd p, the following formula exists [11], being similar to Eq. (B2):

$$\sin^p x \;=\; \frac{1}{2^{p-1}} \cdot \sum_{m=0}^{(p-1)/2} (-1)^{\frac{p-1}{2}-m} \binom{p}{m} \sin\big((p-2m)\,x\big) \qquad \text{(B6)}$$

The term with the central binomial coefficient in Eq. (B2) does not exist here. By replacing x and including the summation over k from Eq. (45), the right side of Eq. (B6) vanishes. The proof is analog to the verification of Eq. (43). We omit the calculation which is straightforward. For the range of definition, the main criterion is the same as before. Thus, Eqs. (45) and (46) are valid for odd p if $(p - 2m)/N$ is not integer for each $m = 0, \ldots, (p - 1)/2$.

Appendix C. Solutions for the "var."-positions in Table 3

A question is if analytical solutions exist also for the gray fields in Table 3, where the results depend additionally on the phase shift α. Actually, equations for any combination of N, p and α were found. We describe this in more detail, but we have to admit that the final formulas seem to be interesting rather from a mathematical point of view than from a physical one.

At first, we provide solutions for all of the "gray" positions to the right of the red line in Table 3, meaning $p/2 < N \le p$. As before, they are split into the cases "even p" and "odd p". So, the results depend on N, p and α. Again, the angle α can be any real number.

The following two equations are valid for the constraints: p even, N even and $N>p/2$. The "±"-sign means "+" if $N \bmod 4 = 0$ ($N = 4, 8, 12, ...$) and "–" if $N \bmod 4 = 2$ ($N = 2, 6, 10, ...$). "Mod" indicates the modulo function.

$$\sum_{k=1}^{N} \sin^p\left(\alpha + \frac{2\pi k}{N}\right) = \frac{N}{2^p}\left(\binom{p}{\frac{p}{2}} \pm 2 \cdot \binom{p}{\frac{p-N}{2}} \cos(N\alpha)\right) \quad \text{(C1)}$$

$$\sum_{k=1}^{N} \cos^p\left(\alpha + \frac{2\pi k}{N}\right) = \frac{N}{2^p}\left(\binom{p}{\frac{p}{2}} + 2 \cdot \binom{p}{\frac{p-N}{2}} \cos(N\alpha)\right) \quad \text{(C2)}$$

For odd p, odd N and $N>p/2$, two corresponding equations were found. Here, the "±"-sign means "+" for $N \bmod 4 = 1$ ($N = 1, 5, 9, ...$) and "–" for $N \bmod 4 = 3$ ($N = 3, 7, 11, ...$).

$$\sum_{k=1}^{N} \sin^p\left(\alpha + \frac{2\pi k}{N}\right) = \pm \frac{N \cdot \sin(N\alpha)}{2^{p-1}} \cdot \binom{p}{\frac{p-N}{2}} \quad \text{(C3)}$$

$$\sum_{k=1}^{N} \cos^p\left(\alpha + \frac{2\pi k}{N}\right) = \frac{N \cdot \cos(N\alpha)}{2^{p-1}} \cdot \binom{p}{\frac{p-N}{2}} \quad \text{(C4)}$$

In order to verify these equations, the singularity 0/0, appearing when applying Lagrange's identities, has to be avoided. This discontinuity can be removed by introducing an infinitesimally small phase shift ε, added each to the term $(p–2m)2\pi/N$ in the arguments of the trigonometric functions in Eq. (B4). With the limiting case $\varepsilon \to 0$, the summation in Eq. (B4) becomes N. By further evaluating Eq. (B3) (or analogously (B6)), the equations (C1) and (C3) can be derived. Equations (C2) and (C4) easily follow from the change α to $\alpha + 90°$. The main aspect of the range $N>p/2$ and of Eqs. (C1)–(C4) is that only one m-term contributes to the result, determined by the condition that $(p-2m)/N$ is integer. We skip further details of the derivation. But what about the area to the left of the red line in Table 3 ($N \le p/2$)? For a few positions, defined by odd p, odd N and $p/3<N<p/2$ (or $2N<p<3N$), Eqs. (C3) and (C4) are still valid. Anyway, for most of the remaining gray fields, the results are more complex because more than one m-term in Eqs. (B3) or (B6) have to be considered.

Following this path, also solutions for the remaining gray fields could be found. If we take into account that $\binom{p}{m} = 1$ for $m = 0$ and $\binom{p}{m} = 0$ for $m < 0$, then the following equations (C5)–(C8) are generally valid not only for all of the "var."-positions in Table 3 but also for the range $N>p$ (even including $p = 0$). In the latter area, they turn into Eqs. (43)–(46), and for $p/2<N \le p$, they can be reduced to Eqs. (C1)–(C4). Equations (C5)–(C8) have been checked numerically per computer and seem to be correct. The only requirement for obtaining valid sums on the right side of these equations, especially valid summation limits, is the constraint "$(p-2m)/N$ integer" within the range of the variable m. For the zero positions to the left of the diagonal in Table 3 ($N<p$, p odd and N even), this condition is never fulfilled. Therefore, Eqs. (C7) and (C8) are not applied here, and, according to Eqs. (45) and (46), the results are set to zero. For $N>p$, Eqs. (C7) and (C8) automatically yield zero for odd p. The given representation of the summation limits is only one possible solution. Other (similar) formulations can also be used.

For even p, we find the following two equations:

$$\sum_{k=1}^{N} \sin^p\left(\alpha + \frac{2\pi k}{N}\right) = \frac{N}{2^p}\left(\binom{p}{\frac{p}{2}} + 2\cdot\sum_{j=r}^{s}(-1)^{\frac{p}{2}-m}\binom{p}{m}\cdot\cos\left((p-2m)\alpha\right)\right) \qquad \text{(C5)}$$

$$\sum_{k=1}^{N} \cos^p\left(\alpha + \frac{2\pi k}{N}\right) = \frac{N}{2^p}\left(\binom{p}{\frac{p}{2}} + 2\cdot\sum_{j=r}^{s}\binom{p}{m}\cdot\cos\left((p-2m)\alpha\right)\right) \qquad \text{(C6)}$$

$$\text{with} \quad r = \frac{p \bmod (qN)}{2}, \quad s = r + \text{floor}\left(\frac{p}{qN}\right) - 1, \quad m = r + \frac{(j-r)\,N}{3-q}$$

$$\text{and} \quad q = 1 + N \bmod 2\,.$$

In the equation for m, the variable j is the summation index. "Floor" indicates the floor function which is similar to the integer function. It yields the largest integer, less than or equal to the real argument (example: floor(–2.4) = –3). The variable q, with $q = 1$ for even N and $q = 2$ for odd N, has been introduced to reduce the number of equations. For odd p, we obtain

$$\sum_{k=1}^{N} \sin^p\left(\alpha + \frac{2\pi k}{N}\right) = \frac{N}{2^{p-1}}\cdot\sum_{j=r}^{s}(-1)^{\frac{p-1}{2}-m}\binom{p}{m}\cdot\sin\left((p-2m)\alpha\right) \qquad \text{(C7)}$$

$$\sum_{k=1}^{N} \cos^p\left(\alpha + \frac{2\pi k}{N}\right) = \frac{N}{2^{p-1}}\cdot\sum_{j=r}^{s}\binom{p}{m}\cdot\cos\left((p-2m)\alpha\right) \qquad \text{(C8)}$$

$$\text{with} \quad r = \frac{(p+N+2-q) \bmod (2N)}{2} \quad \text{and} \quad s = r + \text{floor}\left(\frac{p-N}{2N}\right).$$

The variables m and q are defined above. Again, the summation bounds and m-values (not the main equations) were found empirically. Since different cases concerning these bounds exist, we omit a lengthy derivation. Please notice that the k-summation vanishes on the right side of these equations and that in the majority of cases the number of summands in the j-summation is considerably less than the number of terms in the sum over k.

An easier way to represent Eqs. (C5) and (C6), for example, is to replace the summation $\sum_{j=r}^{s}$ ... by $\sum_{m=0}^{p/2-1}$ ... , with the individual m-terms being taken into account only if $(p-2m)/N$ is integer. This can readily be achieved by checking the condition

$$\text{frac}\left(\frac{p-2m}{N}\right) = 0 \qquad \text{(C9)}$$

The “frac” function returns the fractional part of a number. For Eqs. (C7) and (C8), we would use $\sum_{m=0}^{(p-1)/2}$ ... . That way, the equations for the quantities r, s, m and q are not needed. In addition, Eqs. (C5)–(C8) would be true for all values of N and p, including all of the zero positions in Table 3. At least for computation purposes, this version seems to be more appropriate.

In principle, the check of the condition (C9) can be included in Eqs. (C5)–(C8) by using the signum function "sgn". By considering also the change of the summation bounds, as described before, Eq. (C5) becomes

$$\sum_{k=1}^{N} \sin^{p}\left(\alpha + \frac{2\pi k}{N}\right) = \frac{N}{2^{p}} \binom{p}{\frac{p}{2}} + \frac{N}{2^{p-1}} \cdot \sum_{m=0}^{p/2-1} \left(1 - \operatorname{sgn}\left(\operatorname{frac}\left(\frac{p-2m}{N}\right)\right)\right) \cdot (-1)^{\frac{p}{2}-m} \binom{p}{m} \cdot \cos\left((p-2m)\,\alpha\right) \qquad \text{(C10)}$$

If we treat Eqs. (C6)–(C8) accordingly, we have a set of four equations, yielding solutions for any natural numbers N and p and for any real angle α.

It is interesting that for all corresponding combinations of N and p, a specific formula can be deduced from Eqs. (C5)–(C8) by inserting values for N and p but not for α. (Note that for $N=1$, e.g., Eq. (C7) is reduced to Eq. (B6).) Thus, we provide the two examples: $N=1$, $p=3$ (Eq. (C7), see also [8, 11]) and $N=3$, $p=10$ (Eq. (C6)), leading to the following trigonometric identities.

$$\sin^{3}\alpha = \frac{1}{4} \cdot \left(3\,\sin\alpha - \sin\left(3\,\alpha\right)\right) \qquad \text{(C11)}$$

$$\cos^{10}\alpha + \cos^{10}\left(\alpha + \frac{2}{3}\pi\right) + \cos^{10}\left(\alpha + \frac{4}{3}\pi\right) = \frac{378 + 135\,\cos\left(6\,\alpha\right)}{512} \qquad \text{(C12)}$$

References

[1] John B. Wachtman, W. Roger Cannon, M. John Matthewson, "Mechanical Properties of Ceramics, Second Edition," A John Wiley & Sons, Inc., Publication, Rutgers University, USA, pp. 97, 99 (2009), doi: 10.1002/9780470451519.fmatter.

[2] Christian Spura, "Technische Mechanik 2 – Elastostatik – Nach fest kommt ab," Springer Vieweg, pp. 151–153, 156 (2019), doi: 10.1007/978-3-658-19979-1.

[3] Matthew R. Begley, Daniel S. Gianola, Tyler R. Ray, "Bridging Functional Nanocomposites to Robust Macroscale Devices," Science **364/6447**, eaav4299 (2019).

[4] Elena V. Sturm (née Rosseeval), Helmut Cölfen, "Mesocrystals: Past, Presence, Future," Crystals **7/7**, p. 207 (2017).

[5] Michael A. Boles, Michael Engel, Dmitri V. Talapin, "Self-Assembly of Colloidal Nanocrystals: From Intricate Structures to Functional Materials," Chem. Rev. **116/18**, pp. 11220-11289 (2016).

[6] Berta Domènech, Alvin T. L. Tan, Hans Jelitto, Eduardo Zegarra Berodt, Malte Blankenburg, Oliver Focke, Jaclyn Cann, C. Cem Tasan, Lucio Colombi Ciacchi, Martin Müller, Kaline P. Furlan, A. John Hart, Gerold A. Schneider, "Strong Macroscale Supercrystalline Structures by 3D Printing Combined with Self-assembly of Ceramic Functionalized Nanoparticles," Adv. Eng. Mater. **22/7**, 2000352 (2020), Inside front cover, 2070028 (2020), highlighted also on the "Advanced Science News" web page.

[7] Supplemental material to previous reference (B. Domènech et al.), free download on ResearchGate (RG) via previous paper under "Supplementary resources" or "Linked data": 1. pdf-file, supporting information, 2. real time MP4-video of 3D-printing process, 3. and 4. two MP4-videos of tomographic XRM 3D reconstruction, longitudinal section and cross section (2020).

[8] I. N. Bronstein, K. A. Semendjajew, "Taschenbuch der Mathematik," Harri Deutsch, Thun und Frankfurt/Main, 19. Auflage, pp. 101–102, 235 (1979).

[9] Wolfgang Grellmann, Sabine Seidler, "Kunststoffprüfung (2. Auflage)," Carl Hanser Verlag, München, pp. 148–149 (2011), ISBN: 978-3-446-42722-8.

[10] Eddie Ortiz Muñiz, "A Method for Deriving Various Formulas in Electrostatics and Electromagnetism Using Lagrange's Trigonometric Identities," Am. J. Phys. **21/2**, p. 140 (1953).

[11] Izrailʹ Solomonovich Gradshteĭn (other: Daniel Zwillinger, I. M. Ryzhik, Victor Moll, “Table of integrals, series and products (8th edition),” Waltham, Massachusetts Academic Press, eBook, ISBN 9780123849342, 9780123849335 (2015) pp. 30, 31